Note RD42-4

Results from the RD-42 October '95 Beam Test at CERN

John Conway, Vince Jacobs, Michael Walsh
Rutgers University

24 January 1996

Abstract

Data from the two 50-micron-pitch CVD diamond detectors tested in October at CERN confirm earlier observations and give new information about the effect of radiation on the detectors. The F detector from Norton and the S4 detector from DeBeers show very different behavior, raising questions about the charge transport in the detector and/or the performance on the readout electronics.

1 Overview

In October of 1995 two CVD diamond detectors plated with 50-micron strips were tested at CERN. One, denoted F, is the same detector tested in the July beam test. The other, denoted S4, is based on a diamond sample supplied by DeBeers. Both detectors were equipped with VA-2 readout chips, and tested in the test beam telescope described in notes RD42-2 and RD42-3. Data from both detectors were collected after exposure to levels of ^{90}Sr gamma radiation exposure ranging from 0 to 42 hours. The aims of the test were to confirm the earlier measurements with F and see if the "pump-up" with radiation exposure could be extended, and to test in a beam a the detector from a new diamond sample from DeBeers.

2 Data analysis

Table 1 summarizes the data used in the analysis presented here. The raw data tapes were processed with the program TELANA, resulting in DST files of the same format used for the May and July data. The clusters in the silicon detectors were stored on the DST along with the full diamond plane information. After alignment, micro-DSTs containing only silicon clusters and the region in the diamond planes within five strips of the track extrapolation resulted in a factor of five reduction in size, allowing disk storage of the full data set.

3 Fiducial cuts and alignment

The alignment of the eight silicon planes in the silicon telescope is done using the first 20000 tracks from each run. Cluster are found using the method described in the notes RD42-2

Table 1.
Run Summary

run	Sir 7	Sir 8	exposure	events
211	F (300V)	S4 (500V)	0 h	140,000
212	F (300V)	S4 (500V)	0 h	140,000
213	F (300V)	S4 (500V)	0 h	140,000
219	F* (300V)	S4* (500V)	17 h	138,000
220	F* (300V)	S4* (500V)	17 h	135,000
222	F** (300V)	S4** (500V)	28 h	128,000
223	F** (300V)	S4** (500V)	28 h	125,000
224	F** (300V)	S4** (500V)	28 h	140,000
265	F*** (300V)	S4*** (500V)	42 h	140,000
266	F*** (300V)	S4*** (500V)	42 h	140,000
267	F*** (300V)	S4*** (500V)	42 h	140,000

and RD42-3. The "good" hit clusters used throughout the alignment procedure comprise strips which are not dead or noisy. The strip with the greatest charge and its two immediate neighbors must have rms noise in the range of 0.5 to 6.0 ADC counts, for the silicon planes, or 0.5 to 5.0 ADC counts for the case of the diamond planes.

The hit with the greatest charge in each silicon plane is used in a least χ^2 track fit to a straight line. The fit returns corrections to the initial offsets and rotations describing the alignment of each silicon plane. The final iteration uses only hits with residuals better than twenty microns.

After alignment of the silicon telescope, the tracks are extrapolated into the diamond detectors. All tracks in a run are used to align the diamond planes. Good hit clusters found in the diamond are matched with the tracks extrapolated from the silicon telescope. The residual distance between the hit and the track is plotted as a function of position in the diamond plane, and this plot is used to compute corrections to the diamond plane alignment. The resulting run-by-run alignment is stable to better than a micron for the F detector, and to a few microns for the S4 detector. At this level uncertainties in the alignment do not contribute significantly to the observed resolution of the diamond detectors.

The track residuals as a function of position (in the direction across the strips) are shown in figure 1 for both the F and S4 detectors. Here the top plot for each detector shows all residuals immediately after alignment. Dead and noisy regions of the detector are included in this plot. The middle plot shows the residuals after a [0.5, 5.0] rms noise cut has been placed on the diamond strip through which the extrapolated track passes and on the neighboring strips. Finally, the bottom plot shows the residuals after fiducial cuts have been placed on the extrapolated track defining the diamond detector's good regions. Only tracks in these fiducial regions will be used in the rest of the analysis.

Figure 2 shows the residuals for the F and S4 detectors as a function of position along the strip. F shows a clear broadening at the end of the strip. In the case of S4 this is less clear. The strip ends are excluded from the fiducial regions.

Figure 3 shows the fiducial regions in the diamond detectors. The fiducial areas cover most of the F detector; only small parts of S4 can be used for further study.

To verify whether the z-positions of the diamond detectors are correct, one can plot the hit

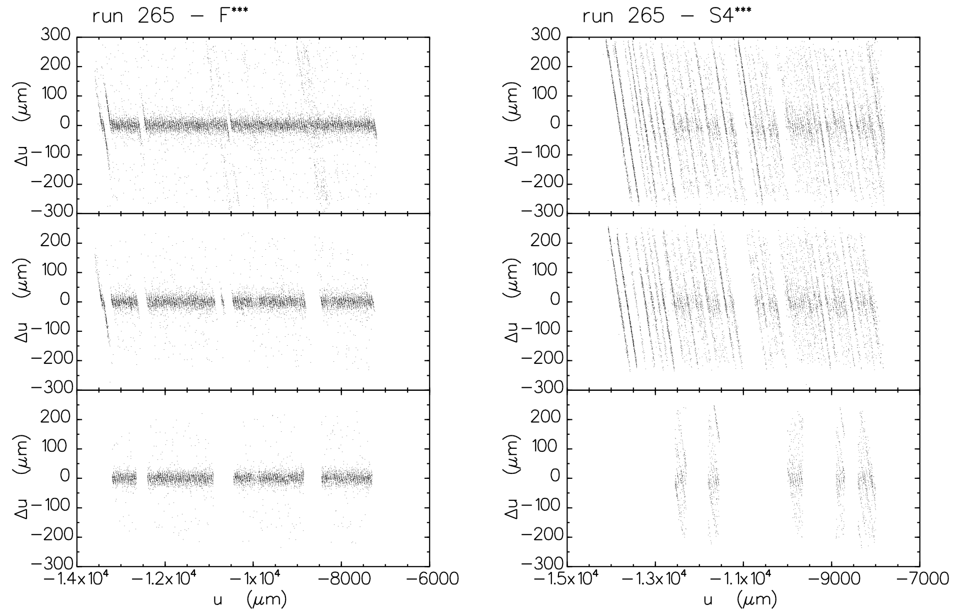

Figure 1: Hit position minus track position Δu in the F and S4 detectors versus track u position. The top plot shows the situation after the alignment of the diamond detectors. The middle plot shows it after rms cuts have been placed on the diamond strips nearest the extrapolated track. The bottom plot is after fiducial cuts have been placed on the u and v track positions.

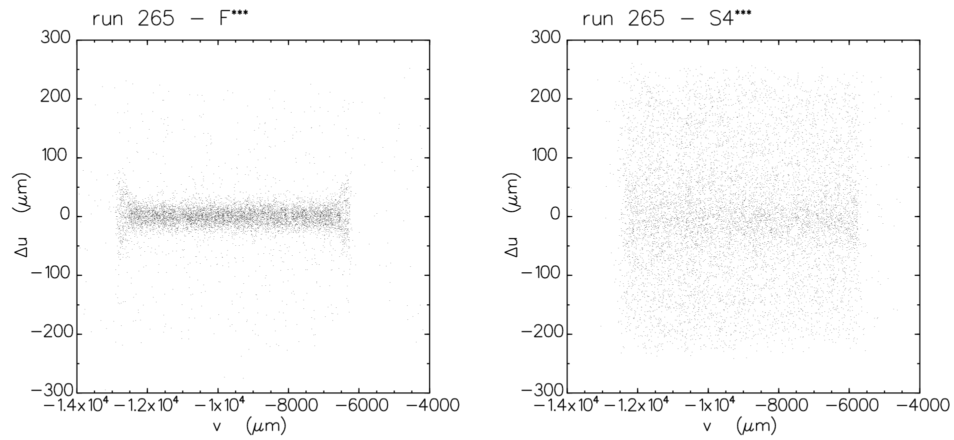

Figure 2: Hit position minus track position Δu in the F and S4 detectors versus track v position. The F detector shows a clear broadening at the ends of the strip. This is less clear for the S4 detector.

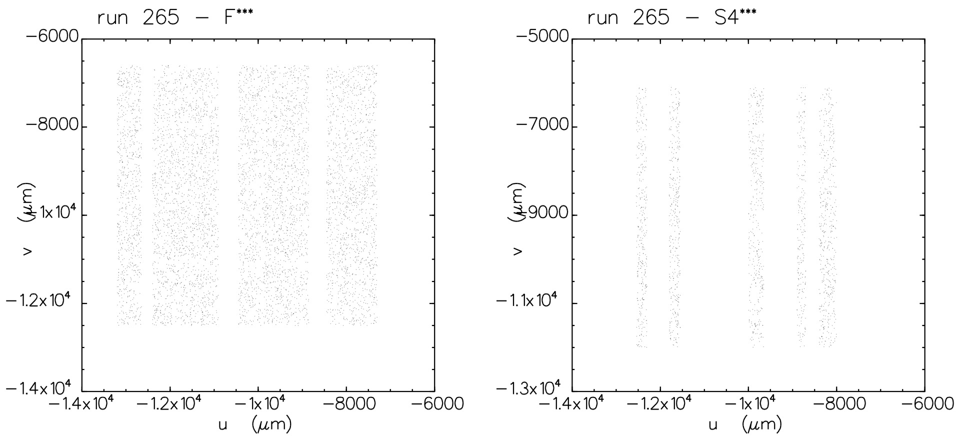

Figure 3: Uniform illumination of the fiducial regions in the F and S4 detectors. The faint horizontal features are due to bad channels in the silicon telescope.

deviation Δu versus an arbitrary z offset, and see if the rms of Δu as a function of Δz has a minimum at $\Delta z = 0$. Figure 4 shows these distributions for the two detectors; the F detector has a clear minimum at Δz=0, and the minimum for the S4 detector, though less clear, is also consistent with Δz=0.

4 Clustered analysis

The cluster algorithm used in this analysis differed slightly from the two-strip algorithm used in the analysis of previous beam tests. In the earlier tests clusters were formed from the strip with largest pulse height and the higher of the two adjacent strips. In this analysis, the other adjacent strip is also used in the cluster if its pulse height is either more than two sigma larger than 0 or if its pulse height is within 2 sigma of the pulse height of the other adjacent strip. This modification avoids the case where there is some ambiguity as to which adjacent strip to use.

This so-called "2/3-strip" algorithm estimates the cluster charge from the sum of the pulse heights on all used strips, and estimates the cluster position from the pulse-height-weighted sum of the strip positions.

The position resolution of the F detector shows no qualitative change from the July measurement. Figure 5 shows the correlation of Δu with fractional strip position s. The figure also shows the rms of the Δu distribution as a function of s. As was the case in the July measurement, the correlation which appears as stripes in the plots means that the resolution is intrinsically non-Gaussian. The plots of the rms of Δu, labelled σ_u, show minima at the center of the strips (s = 0 or 1), increasing smoothly to an rms about 50% larger in between the strips (s = 0.5). The distributions after radiation exposure are essentially the same, and have a slightly larger σ_u.

Note that the shape of the distribution for the unpumped detector differs from that observed in the July test (cf. note RD42-3, figure 7). The source of the difference is the change in the cluster algorithm. Here, when the track projects to the strip center, using the 2/3-strip algorithm tends to make $\Delta u = 0$ since the algorithm tends to use the third strip. This was not

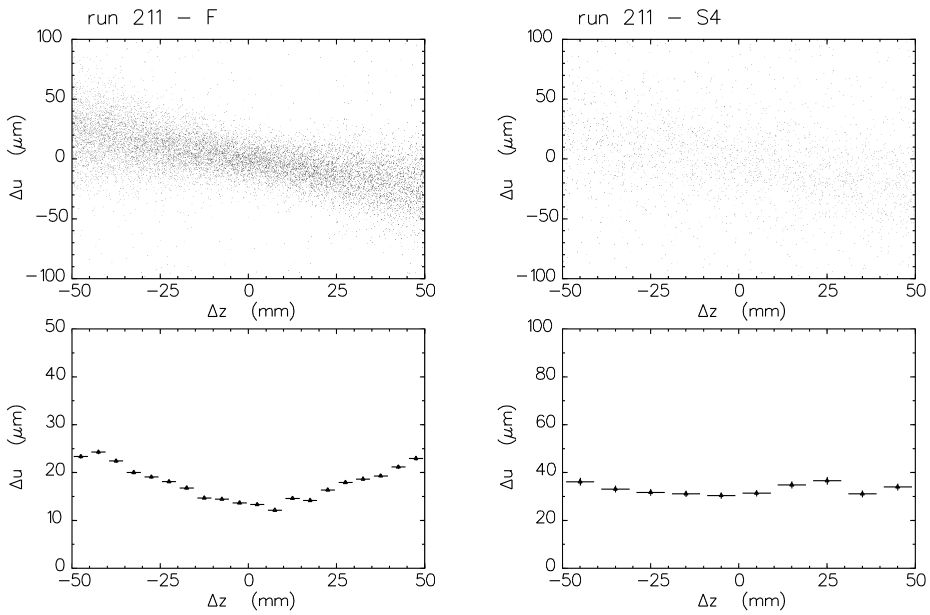

Figure 4: Hit position minus track position Δu in the F and S4 detectors versus an arbitrary z offset Δz. The lower plots show the rms of the vertical axis as a function of Δz; the minima at Δz=0 indicate that the nominal z positions are accurate.

true for the 2-strip algorithm, which tended to not calculate Δu correctly at the strip center.

For the S4 detector the situation is worse, due to a much smaller amount of collected charge. (See below.) Figure 6 shows the distribution of Δu versus s; the resolution is completely dominated by the effects discussed below.

5 Transparent analysis

The transparent analysis allows study of the charge collected in the detector. In this case the track must project to a fiducial region of the detector, to strips with noise (rms) of between 0.5 and 7 ADC counts. No track is used if any of the silicon plane hits deviate by more than 10 μm from the track.

Over how many strips is the charge deposited? Figure 7 shows the distribution of charge collected on the central three and five strips as a function of radiation exposure. In fact for the unexposed F detector the five-strip summed charge has a mean about 10% larger than that of the three-strip charge. This ratio, however, does not persist into the high-exposure runs, which have comparable mean charge. Furthermore, after the first 17-hour exposure the mean of the charge distribution stays roughly constant.

The mean charge versus fractional strip position s, shown in figure 8 has a "dip" of about 10% in the region between the strips, s = 0.5. This effect appears in both the three- and five-strip charge sums, but is less pronounced in the five-strip case.

A more serious effect appears when the mean charge is plotted as a function of event sequence number (time into the run). Figure 9 shows the mean charge versus a number

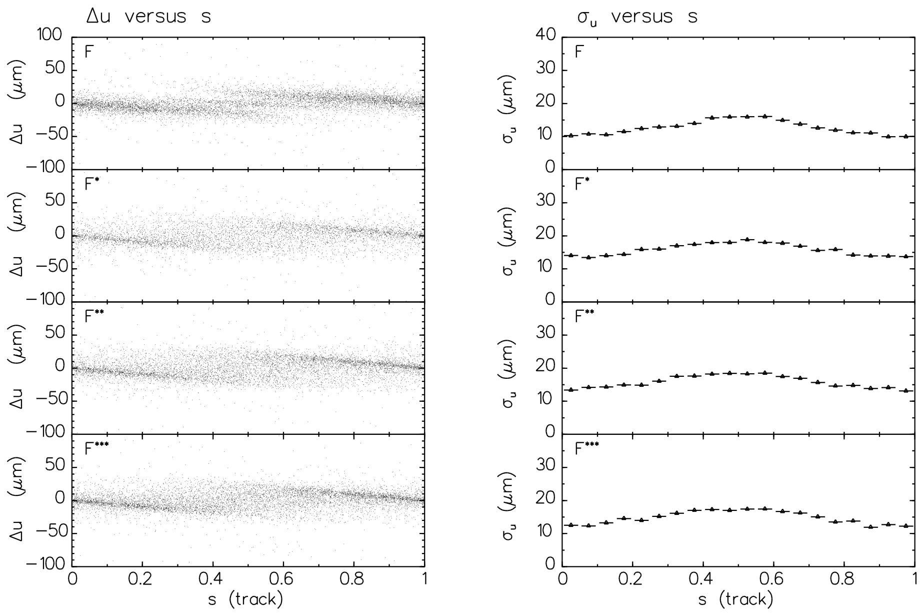

Figure 5: Hit position minus track position Δu versus fractional strip position s in the F detector for the various radiation exposure levels. The right-hand plots show the rms of the Δu distribution as a function of s

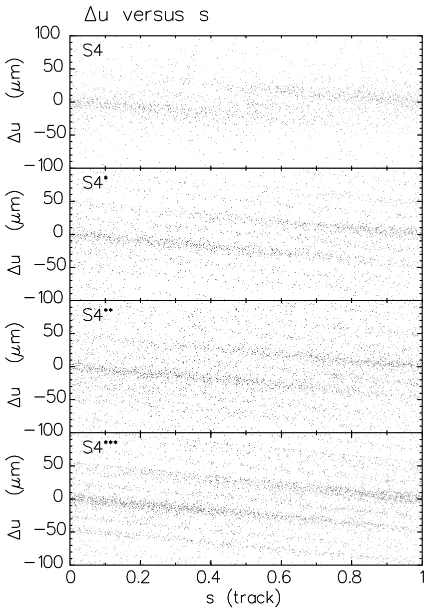

Figure 6: Hit position minus track position Δu versus fractional strip position s in the S4 detector for the various radiation exposure levels.

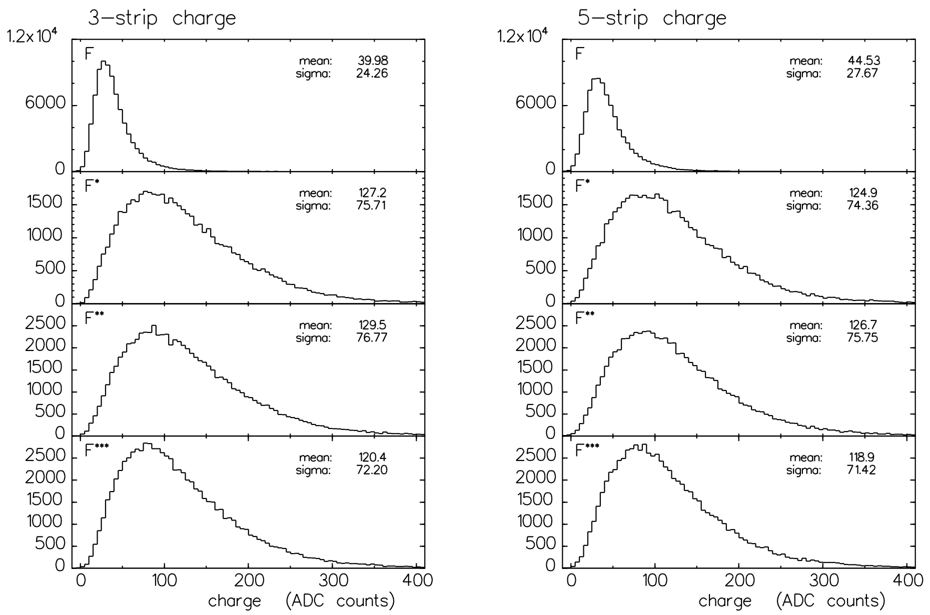

Figure 7: Summed charge in three- and five-strip region around extrapolated track position in the F detector.

calculated as [run number + (event number/140,000)], labelled "run.event." For the three run groups with radiation exposure (F*, F**, and F***) the mean charge decreases with time into the run. The effect is larger for the higher-exposure run groups. This could potentially be due to thermal "de-pumping" of the diamond from the pumped state; indeed, after each exposure the diamond appears to be reset to a mean charge near 130 ADC counts.

Do the data exhibit the other effect observed in the July '95 data wherein the pulse height on the strips adjacent to the central strip (the strip nearest the extrapolated track) tend toward negative values as the central strip pulse height increases? The answer, as shown in figure 10, is yes. Indeed the plots show that the effect is just as observed in the July data (cf. RD42-3, figure 9). The figure also shows that the correlation persists for several channels; in fact the strip two strips away from the central strip on one side is correlated with the strip two strips away from the central strip on th other side. Furthermore the plot shows that most often both strips are in fact negative.

The analogous plots for the S4 detector appear in figures 11 through 9. The S4 detector has a much smaller charge, even after radiation exposure, shows no sign of a "dip" in mean charge between strips, and little or no decrease in mean charge with time.

However the comparison of three- and five-strip charge, and the the strip-to-strip correlation plots show that the correlation goes in the opposite direction: the adjacent and next-to-adjacent strips are strongly positively correlated with each other and the central strip pulse height.

Several possibilities present themselves as an explanation for this effect:

1. There is some physical phenomenon in the diamond bulk which affects the charge sharing in such a way as to induce either positive or negative correlations.
2. The VA-2 electronics have crosstalk which can either result in positive or negative corre-

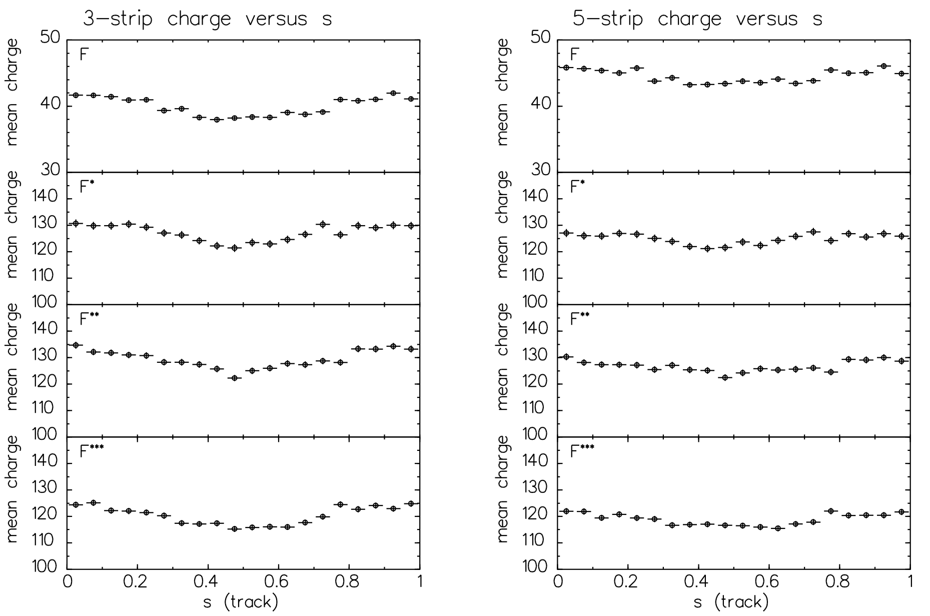

Figure 8: Mean of summed charge in three- and five-strip region around extrapolated track position in the F detector versus fractional strip position s.

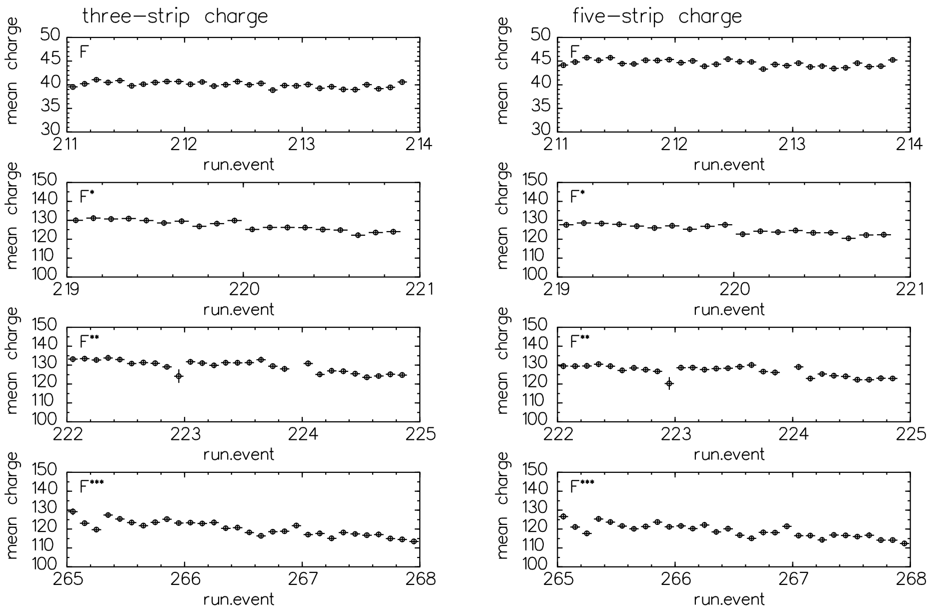

Figure 9: Mean of summed charge in three- and five-strip region around extrapolated track position in the F detector versus run sequence number.

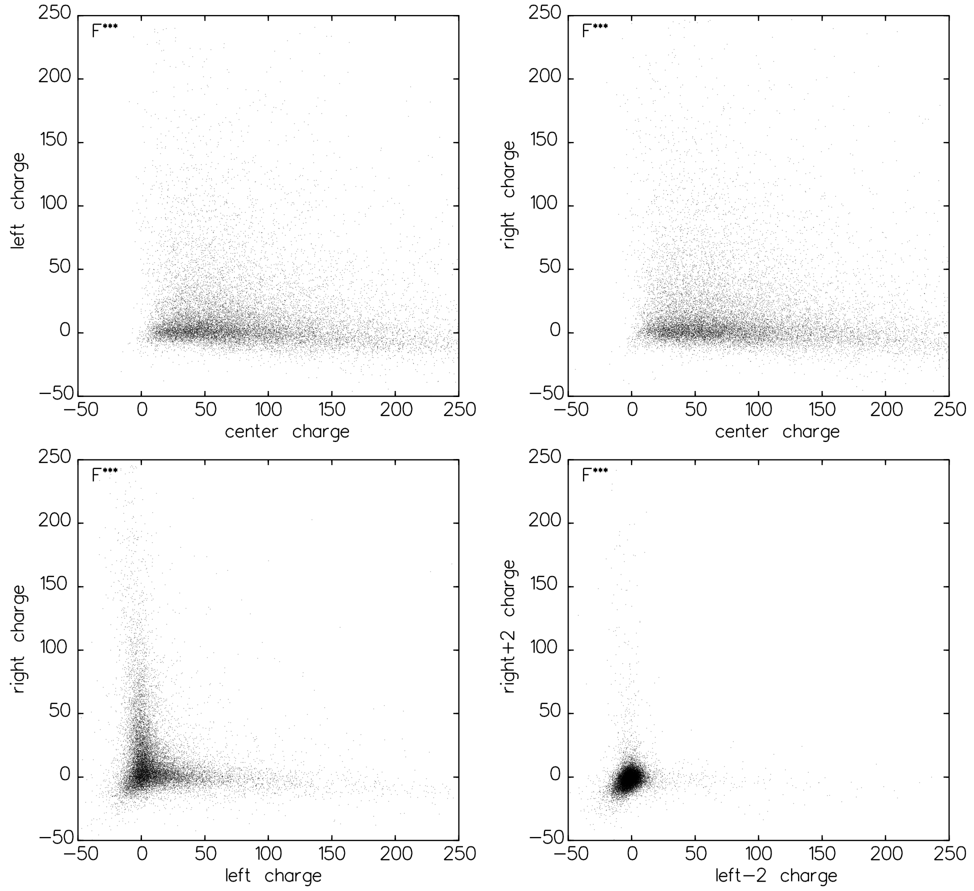

Figure 10: Correlations between pulse heights in five-strip region near extrapolated track position for the F** detector

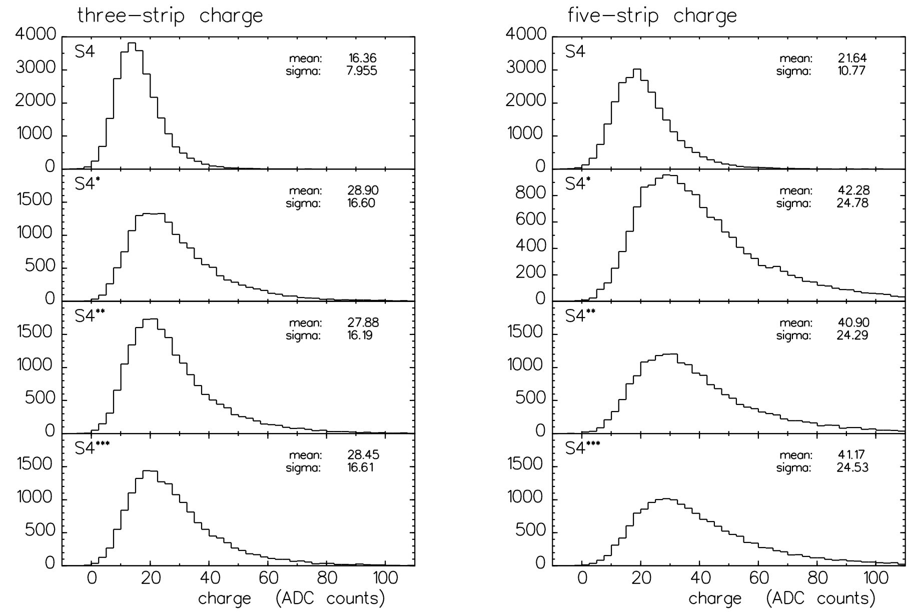

Figure 11: Summed charge in three- and five-strip region around extrapolated track position in the S4 detector.

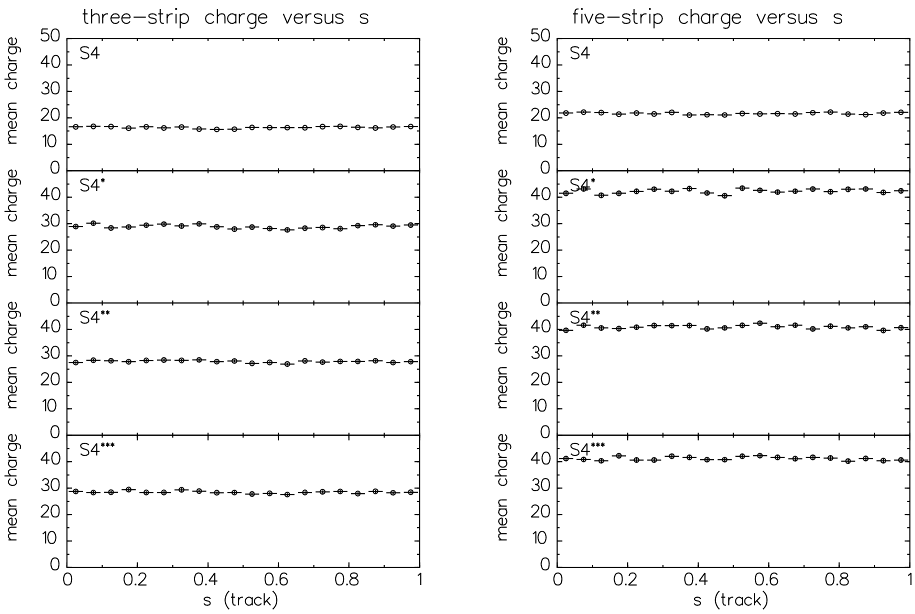

Figure 12: Mean of summed charge in three- and five-strip region around extrapolated track position in the S4 detector versus fractional strip position s.

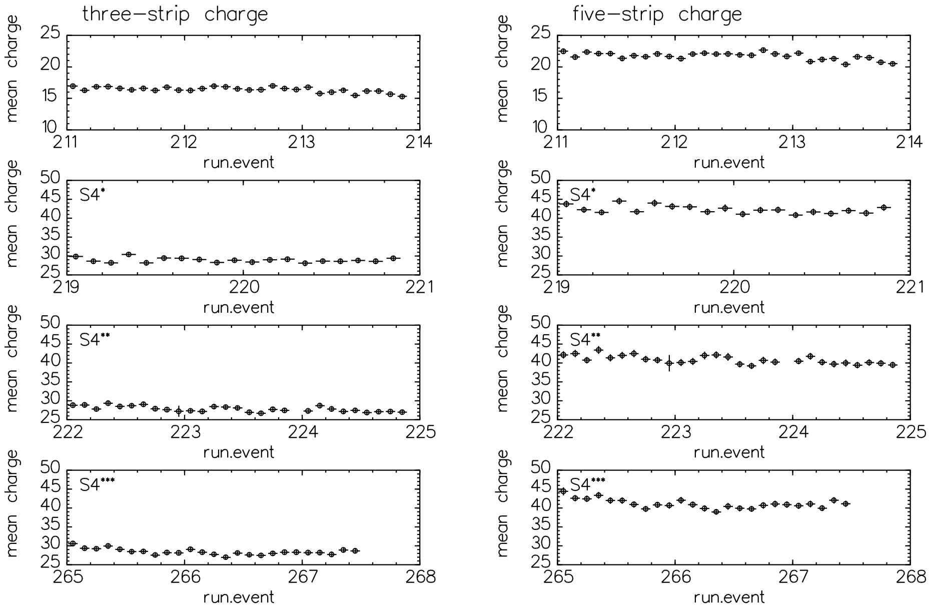

Figure 13: Mean of summed charge in three- and five-strip region around extrapolated track position in the S4 detector versus run sequence number.

lations depending on the chip control voltages.

3. Some software problem related to the common-mode and/or pedestal calculation induces a positive or negative correlation depending on the presence of intermittently noisy or stuck channels.

To decide among these possibilities requires a deeper inspection of the pulse shapes.

Figure 15 shows an unbiased sample of pulses from run 265, for the F and S4 detectors respectively. The plots show graphically the pulse height on each of the eleven strips nearest the strip through which the track passed. The arrow indicates the projected track position. The figures clearly indicate that the negative correlations in F** and the positive correlations in S** extend out several strips (to nearly 200 μm!) on either side of the central strip.

If possibility 3 above is correct, that a software problem in the common mode correction accounts for the effect, then the correlation should persist out to the whole detector plane. However, the event displays in figures 16 and 17 would suggest that the correlation dies out after five or six strips. This tends to rule out a problem in the common mode correction.

Left with either the possibility of a physical detector phenomenon or electronics crosstalk, the latter seems much more likely. Bench tests of the electronics may be able to reveal the source of the crosstalk. Also, a future beam test could help shed light on the question if a silicon detector were to be equipped with identical electronics, and tested in the same manner as the diamond detectors.

Did the effect exist in the July test? Figure 18 shows four selected events from run 424. In this run were present the D, F, and X detectors. As in the October data, the F detector shows a clear negative-going correlation of the channels near the central strip to the central strip. The pulse shapes of the D detector (from DeBeers) show positive correlation similar to

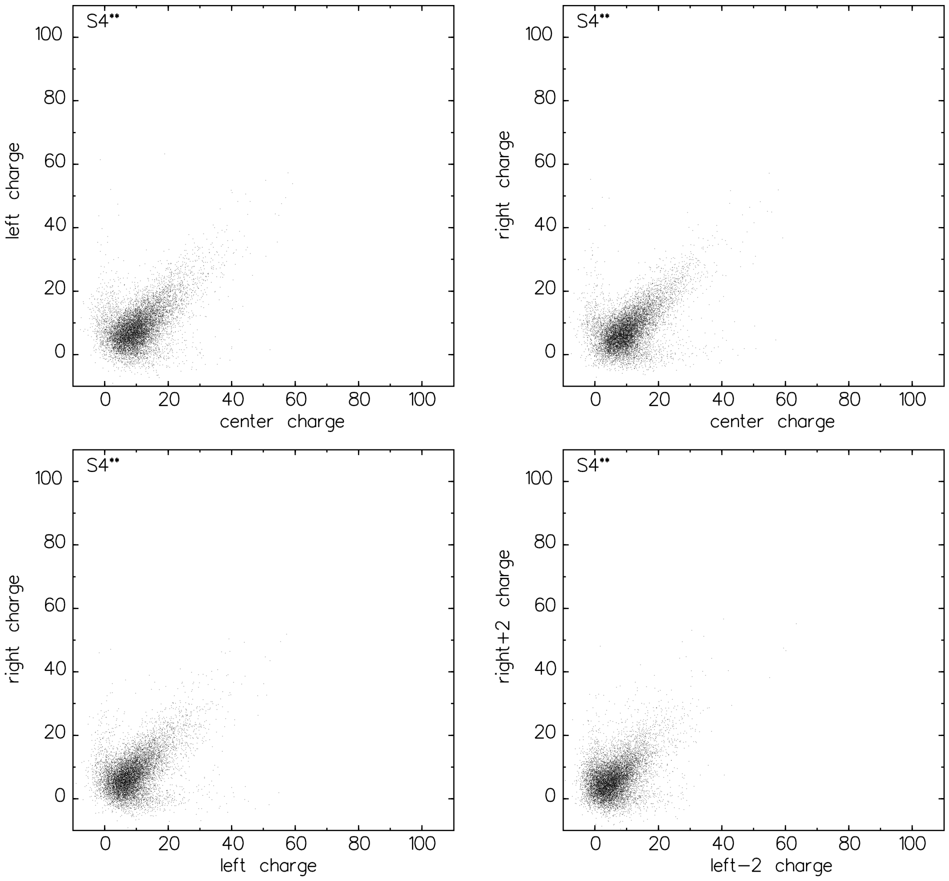

Figure 14: Correlations between pulse heights in five-strip region near extrapolated track position for S4** detector

the S4 detector. The X detector (from Norton) also shows positive correlation, but to a lesser extent.

6 Discussion and Conclusions

The data presented in this note raise many questions. Given that the F detector shows what appears to be strong negative "crosstalk," can one reliably use the data to measure the collected charge? Likewise the S4 detector either suffers from extremely large charge "spreading" (up to several hundred microns) or from the same electronic "crosstalk" but with opposite polarity. Bench tests may reveal whether the source of this effect lies in the electronics or the physics of charge transport in the detector. Equipping a silicon detector with VA-2 electronics would allow one to categorically rule out the detector if the effect is also observed in the silicon case.

Is the fact that the F detector shows 10% charge loss in the interstrip region, whilst the S4 detector shows no loss a clue to the origin of the "crosstalk" effect? Or would one expect such an effect from electronic crosstalk?

Similarly, the fact that the mean charge decreases with time either reflects some time-dependence in the readout electronics or in the detector. The fact that the decrease does not appear to affect the detector in the unpumped state tends to rule out a time-dependent calibration effect. In future beam tests the detector temperature should be recorded with the event records.

In the July beam test the F detector appeared not to have saturated after the maximum exposure to the ^{90}Sr source. In this beam test, however, it saturated at around 120 ADC counts after the first exposure. In future beam tests one should attempt to measure in a quantitative way the dose received by the detectors. In any case the NDF_005 wafer from which F was made had contamination which means that it is not foreseen as a viable detector material.

As stated above the S4 detector from DeBeers either has very wide charge spreading and large charge collected, or small charge collected and wide pulses due to electronic crosstalk. In either case the resulting poor position resolution means that further improvements are necessary before the material and/or electronics could successfully be applied in an actual detector.

Acknowledgements

This document represents not only our work but the enormous effort of the members of RD42 who made the beam test happen, and made it a success. We thank them all for their dedication to this project.

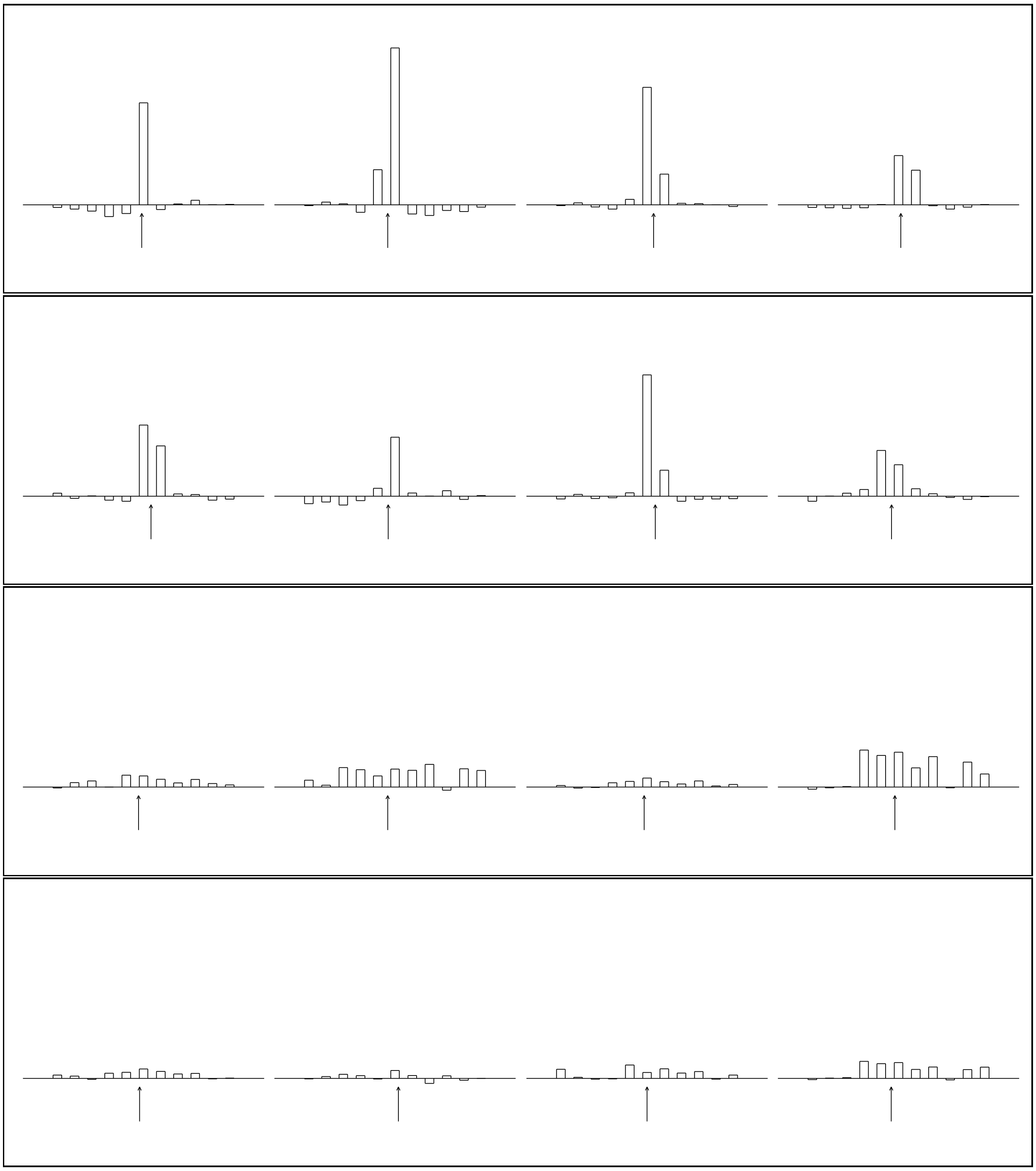

Figure 15: Typical pulses in the F detector (top two boxes) and the S4 detector (bottom two boxes). The arrow indicates the extrapolated track position. The pulses from strips within five strips of the central strip are shown.

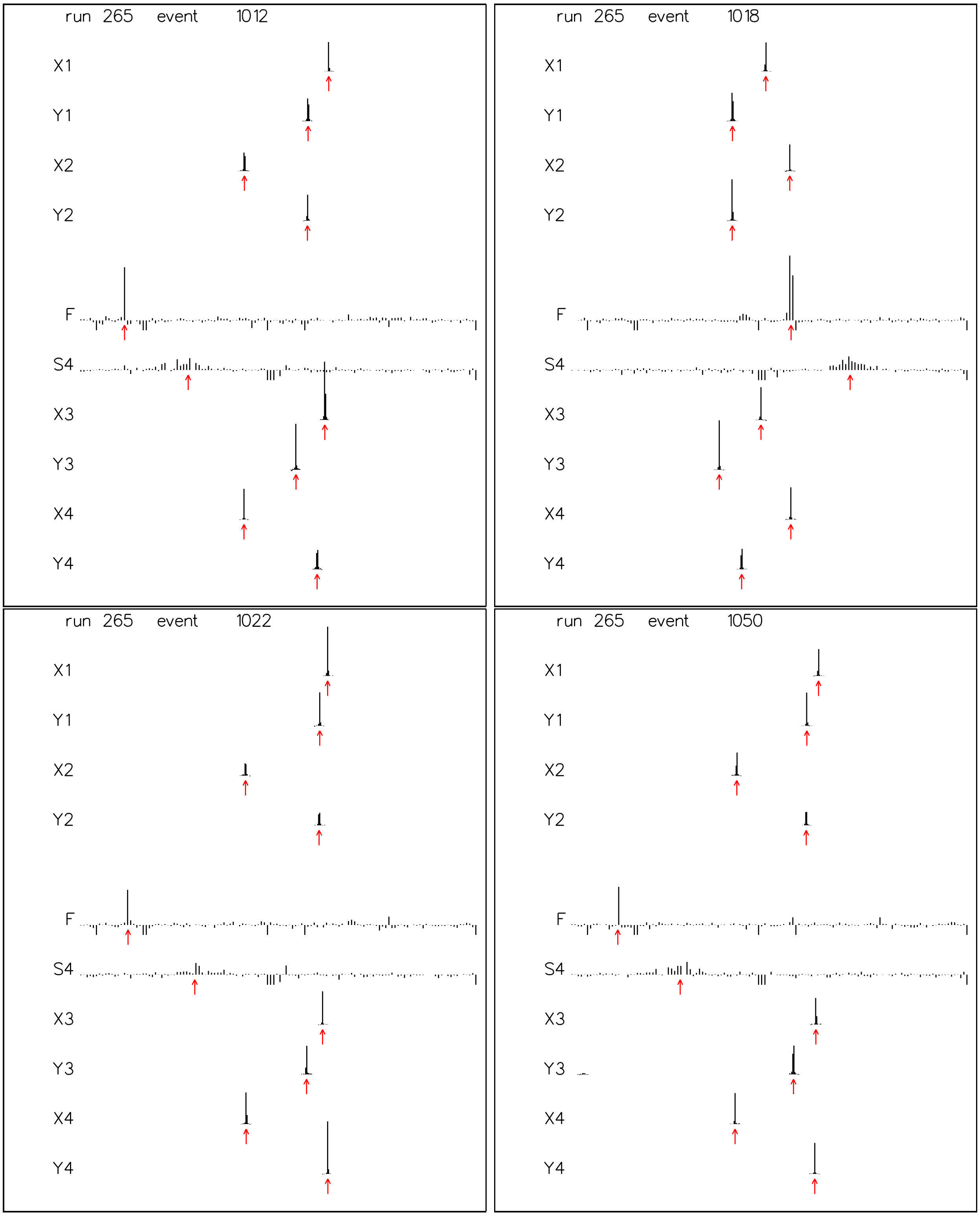

Figure 16: Full event displays from run 265, for tracks projecting into the fiducial regions of both diamond detectors.

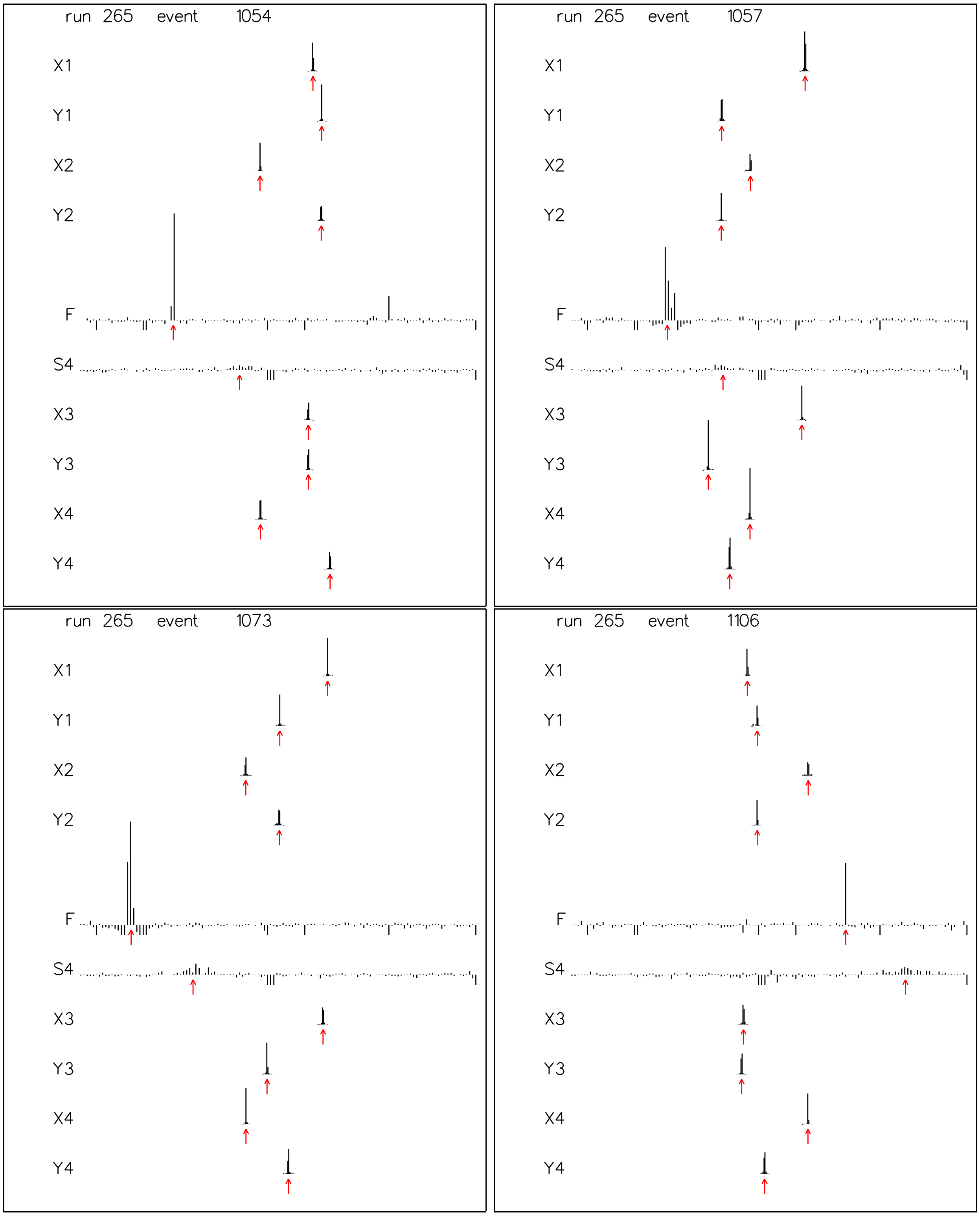

Figure 17: Full event displays from run 265, for tracks projecting into the fiducial regions of both diamond detectors.

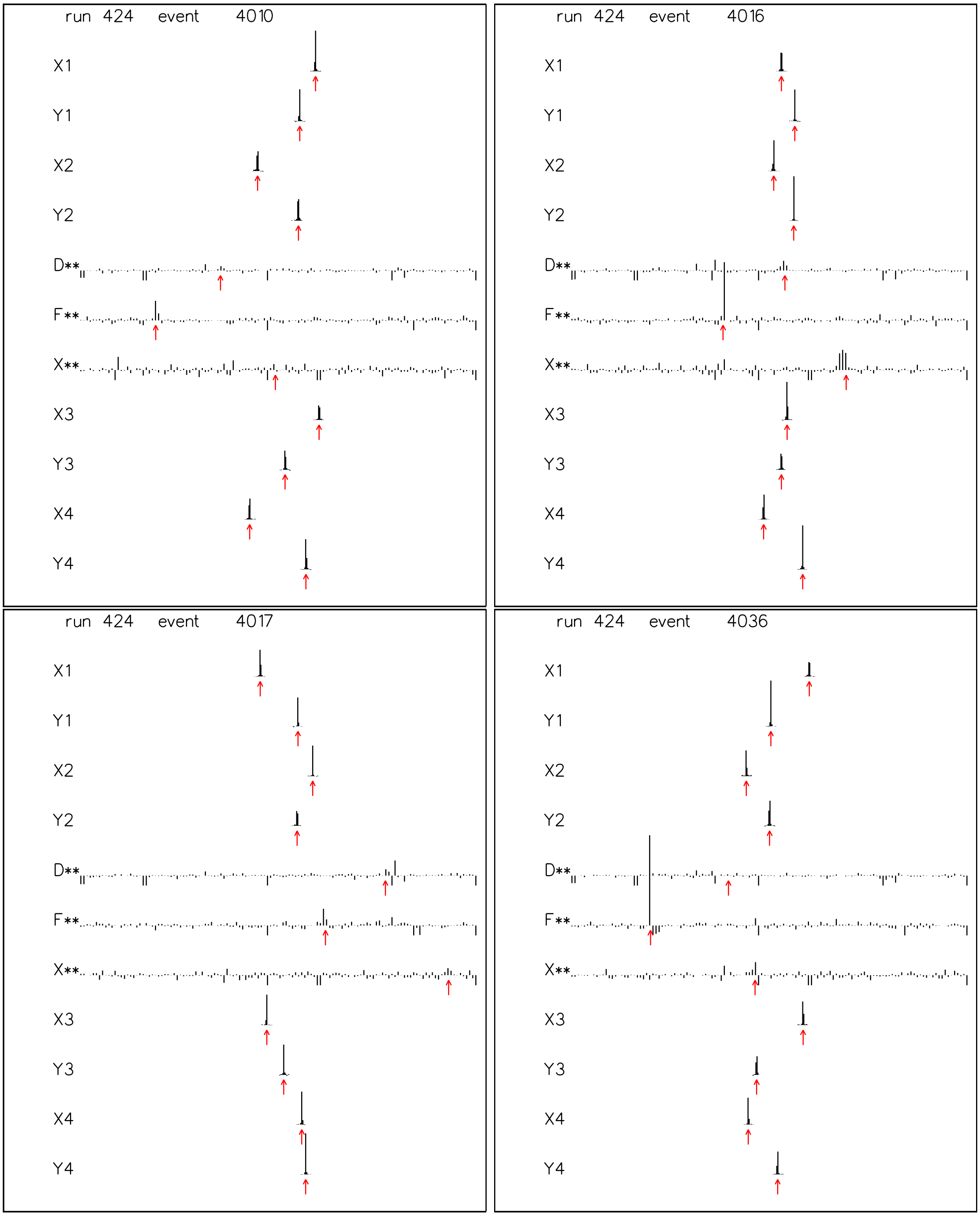

Figure 18: Full event displays from run 424 in the July test.